HHS Public Access

Author manuscript

Mol Cell Endocrinol. Author manuscript; available in PMC 2022 March 15.

Published in final edited form as:

Mol Cell Endocrinol. 2021 March 15; 524: 111169. doi:10.1016/j.mce.2021.111169.

The Bromodomain Containing 8 (BRD8) Transcriptional Network in Human Lung Epithelial Cells

James A. Browne[1,^], **Monali NandyMazumdar**[1,+], **Alekh Paranjapye**[1,+], **Shih-Hsing Leir**[1,2], **Ann Harris**[1,2,*]

[1]Department of Genetics and Genome Sciences, Cleveland, OH, USA

[2]Case Comprehensive Cancer Center, Case Western Reserve University School of Medicine, Cleveland, OH, USA

Abstract

Mechanisms regulating gene expression in the airway epithelium underlie its response to the environment. A network of transcription factors (TFs) and architectural proteins, modulate chromatin accessibility and recruit activating or repressive signals. Bromodomain-containing proteins function as TFs or by engaging methyltransferase or acetyltransferase activity to induce chromatin modifications. Here we investigate the role of Bromodomain Containing 8 (BRD8) in coordinating lung epithelial function. Sites of BRD8 occupancy genome-wide were mapped in human lung epithelial cell lines (Calu-3 and 16HBE14o-). CCCTC-Binding Factor (CTCF) was identified as a predicted co-factor of BRD8, based upon motif over-representation under BRD8 ChIP-seq peaks. Following siRNA-mediated depletion of BRD8, differentially expressed genes with nearby peaks of BRD8 occupancy were subject to gene ontology process enrichment analysis. BRD8 targets are enriched for genes involved in the innate immune response and the cell cycle. Depletion of BRD8 increased the secretion of the antimicrobial peptide beta-defensin 1 and multiple chemokines, and reduced cell proliferation.

Keywords

ChIP-seq; RNA-seq; differential gene expression; transcriptional network

[*]To whom correspondence should be addressed: ann.harris@case.edu.

[^]Current address: Department of Pediatrics, Yale University School of Medicine, New Haven, Connecticut, USA.

[+]These authors contributed equally.

Author Contributions

J.B., M.N., A.P., and A.H. designed the study; J.B., M.N., A.P., S-H.L. and A.H. acquired, analyzed and interpreted data. J.B. and A.H. drafted the article. All authors revised and approved the article.

Genome-wide data are deposited at GEO:
https://www.ncbi.nlm.nih.gov/geo/query/acc.cgi?acc=GSE158688 Enter token kpwxwkqevpirvmp into the box

Introduction

The airway epithelium provides a barrier to inhaled challenges and participates in the regulation of innate immune responses to these insults. Disruption of epithelial integrity underlies several chronic lung diseases, including cystic fibrosis (CF), idiopathic pulmonary fibrosis (IPF) and chronic obstructive pulmonary disease (COPD). Mechanisms that regulate gene expression in the airway epithelium coordinate its response to the environment, both in normal and disease states. The transcriptional network in the airway epithelium has been well-studied during development, primarily in rodents (reviewed in Herriges and Morrisey (2014), and these data provide a valuate framework for understanding the role of specific transcription factors (TFs) in the human lung epithelium. The pivotal role of the pioneer TF Forkhead box A1 (FOXA1) (Paranjapye, Mutolo, Ebron et al., 2020) and of Ets homologous factor (EHF) (Fossum, Mutolo, Yang et al., 2014), in coordinating processes that maintain the integrity of the airway epithelial barrier and its response to injury were reported recently. Moreover, FOXA1 was shown to directly activate SAM pointed domain-containing ETS transcription factor (*SPDEF*) gene expression and repress HOP homeobox (*HOPX1*) and E74-like ETS transcription 5 (*ELF5*) genes in primary human bronchial epithelial cells (Kerschner, Paranjapye, Yin et al., 2020). EHF also directly represses *HOPX1*, Krüppel-like factor 5 (*KLF5*) and retinoic acid receptor beta (*RARB*) expression in these cells. FOXA1 and EHF also regulate each other (Fossum, Mutolo, Tugores et al., 2017), illustrating the complexity of the individual transcriptional networks.

These networks are also coordinated by proteins other than classical transcription factors, for example the Bromodomain-containing proteins (BCPs), which have multiple roles in regulating gene expression both alone or within larger protein complexes. The underlying mechanisms may involve direct regulation of transcription, but more commonly act through histone recognition and modification, and chromatin remodeling (reviewed in (Fujisawa and Filippakopoulos, 2017)). Many BCPs are extremely well-characterized epigenetic readers, which bind to acetylated lysines in histone tails, and provide targets for cancer therapeutics (reviewed in (Perez-Salvia and Esteller, 2017)).

Bromodomain containing 8 (BRD8) is thought to be a nuclear receptor co-activator as it interacts with the thyroid hormone receptor (THR) and augments thyroid hormone-dependent activation of gene expression from thyroid response elements (TREs) in a ligand-dependent manner (Monden, Wondisford and Hollenberg, 1997). However, BRD8 is not well studied in the context of the airway epithelium. Our previous work identified (BRD8) as a potential repressor of the cystic fibrosis transmembrane conductance regulator (*CFTR*) gene (Mutolo, Leir, Fossum et al., 2018), which is mutated in cystic fibrosis. In order to better understand the mechanisms underlying this repression, our goal was to determine the BRD8 transcriptional network in the airway epithelium, since this could reveal a direct or indirect effect on the *CFTR* locus. BRD8 was first characterized as “Skeletal muscle abundant protein” (SMAP) (Nielsen, Petersen, Gliemann et al., 1996). In addition to its role at TREs (Monden et al., 1997), BRD8 is a co-activator of the androgen receptor (AR) (Monden et al., 1997,Hosoya, Monden, Fukabori et al., 2008,Jiang, Ruan, Wang et al., 2016) and the 9-cis-retinoic acid receptor (RXR) in peroxisome proliferator-activated receptor-gamma (PPARγ)/RXR heterodimers (Monden, Kishi, Hosoya et al., 1999), and regulates

PPARγ-target genes during adipogenesis (Couture, Nolet, Beaulieu et al., 2012). BRD8 is also an accessory subunit of the NuA4 histone acetyltransferase (TRRAP/TIP60) complex (Doyon, Selleck, Lane et al., 2004), a complex responsible for acetylation of the N-terminal tails of histone H4 and H2A in yeast. An expanding literature describes a cancer-associated role for BRD8 (reviewed in (Fujisawa and Filippakopoulos, 2017))(Jiang et al., 2016,Yu, Chen, Mo et al., 2020) and a function in the maintenance of genome stability (Lashgari, Fauteux, Marechal et al., 2018). Here, we investigate the role of BRD8 in coordinating gene expression and key biological processes in the normal human lung epithelium. Our studies suggest that BRD8 regulates genes and pathways involved in the innate immune response of lung epithelial cells.

Materials and Methods

Cell culture and RNAi-mediated knockdown of BRD8

Calu-3 (Shen, Finkbeiner, Wine et al., 1994) and 16HBE14o- (Cozens, Yezzi, Kunzelmann et al., 1994) cells were cultured in Dulbecco's Modified Eagle's Medium with 10% fetal bovine serum. Both Dharmacon and Ambion siRNAs (Suppl. Table S-I) were used. Reverse transfections of cells (25,000, 125,000 or 250,000) with siRNA (6, 30 or 60 pmol) were performed in multi-well plates (96, 24 or 12-well plates, respectively) using Lipofectamine RNAiMax (ThermoFisher). Seventy-two hours after transfection, cells were washed in PBS and lysed in TRIzol® (LT) for RNA extraction or in NET Buffer for whole cell lysate (Leir and Harris, 2011).

RNA-seq

The quality of RNA from three replicates of control- and BRD8-siRNA transfected cells was confirmed by Nanodrop measurement of OD 260/280 and 260/230 ratios and by Tapestation. RNA-seq libraries were prepared from 1 μg of total RNA using the TruSeq RNA Sample Preparation Kit v2 per the manufacturer's Low-Throughput protocol (Illumina). Libraries were sequenced on an Illumina HiSeq4000 machines. Raw reads were aligned with STAR 2.6 (Dobin, Davis, Schlesinger et al., 2013) (https://github.com/alexdobin/star). Aligned reads were then assigned to genomic features using featureCounts version 1.6.3 in the Subread package (https://subread.sourceforge.net) (Liao, Smyth and Shi, 2014) and differential gene expression was analyzed using DESeq version 1.22.1 (https://www.bioconductor.org/packages/release/bioc/html/DESeq2.html) (Love, Huber and Anders, 2014). All data are deposited at GEO: GSE 158688

Chromatin immunoprecipitation (ChIP)-seq

Chromatin was prepared from Calu-3 and 16HBE4o- cells as described previously (Browne, Harris and Leir, 2014) and snap frozen in liquid nitrogen. Chromatin immunoprecipitation (ChIP)-seq was performed in 2 biological replicates with an antibody specific for BRD8 (Active Motif 61007) and CTCF (Millipore 07–729). Libraries were generated by standard protocols as described previously (Fossum et al., 2014) and sequenced on an Illumina HiSeq4000 machine. Initial raw reads for the Calu-3 BRD8 were processed using the AQUAS Transcription Factor and Histone ChIP-Seq processing pipeline (https://github.com/kundajelab/chipseq_pipeline) according to the ENCODE (phase-3) guidelines on the hg19

reference genome. This includes mapping using Bowtie2 and peak calling with MACS2. All subsequent dataset processing was done using the WDL-based ENCODE Transcription Factor and Histone ChIP-Seq processing pipeline (https://github.com/ENCODE-DCC/chip-seq-pipeline2). All steps of this pipeline are identical to the previous analysis with the exception of BWA as the mapping software. IDR (Irreproducible Discovery Rate) analysis was applied to the data in order to identify peaks of high confidence. The ChIP-seq data sets are available on GEO (GEO: GSE 158688). Identification of transcription factor motifs in the data set and peak annotation based on the nearest gene were also performed using HOMER (4.7.2q) (http://homer.ucsd.edu/homer/index.html). Gene Ontology (GO) terms enriched among the nearest genes in the ChIP-seq data were determined using the Database for Annotation, Visualization, and Integrated Discovery (DAVID) (Huang da, Sherman and Lempicki, 2009,Huang da, Sherman and Lempicki, 2009).

Real-time quantitative PCR (RT-qPCR)

The TaqMan® reverse transcription kit (LT) was used to make cDNA from total RNA and RT-qPCR then used to measure gene expression levels (primers listed in Suppl. Table S-II).

Western Blotting

Cells were lysed in buffer containing 1% (vol/vol) protease inhibitor cocktail (Sigma P2714) and western blots performed as described previously (Leir and Harris, 2011) using BRD8 (Active Motif 61007) and β-tubulin (Sigma T4026) antibodies.

Cell proliferation assays

For cell proliferation assays, 10,000 Calu-3 cells were reverse transfected with 5 pmol of Ambion Silencer Select negative control 2 (#4390846) or BRD8 (#4392420) siRNAs in 96 well plates, in triplicate. Cells were fixed using methanol: acetic acid (3:1) every 24 hours and the number of cells in each well was counted after DAPI staining, using the BioTek Lionheart FX automated imager and Gen5 image+ analysis software (BioTek). Three independent biological replicates were performed and the data pooled.

Enzyme-linked immunosorbent assay (ELISA)

Cell culture supernatant from siRNA-transfected cells was collected, cleared by centrifugation at 280 × g for 10 minutes to remove cell debris and the supernatant was stored at −80°C. ELISA kits were used to quantify protein levels of Beta-defensin 1 (PeproTech 900-K202), C-C motif chemokine 5 (PeproTech 900-M33) and C-X-C motif chemokine 2 (PeproTech 900-M120). Standard curves were established using serial dilutions of 1:2 starting with 1000 pg/mL of each target. These assays were performed using the ELISA Buffer Kit (PeproTech 900-K00) according to the manufacturer's protocol.

Results

Genome wide occupancy of BRD8 in airway epithelial cells.

As a first step to understanding the contribution of BRD8 to transcriptional networks in the airway, BRD8 ChIP-seq was performed in two biological replicates of chromatin extracted

from Calu-3 lung adenocarcinoma cells and 16HBE14o- immortalized bronchial epithelial cells. Data from the 2 biological replicates were subjected to irreproducible discovery rate (IDR) analysis to generate a single robust dataset for each cell line. Intersecting the BRD8 ChIP-seq binding sites from both Calu-3 (10,165 sites with peak height >10 from a total of 54,743 sites) and 16HBE14o- (9,504 sites, all called by the default parameters of the pipeline) cells, identified 5,173 sites common to both (Suppl. Fig. S-I). These sites of BRD8 occupancy were then annotated with respect to the nearest gene (using ChIPseeker (Yu, Wang and He, 2015)), identifying 2,859 common genes predicted to be regulated by BRD8 in both the airway epithelial cell lines (Suppl. Fig. S-II). In both Calu-3 and 16HBE14o- cells, the majority of BRD8 binding sites were intergenic or at promoters (< 1kb upstream of the transcription start site). A similar genomic distribution was observed for the 5,173 sites found in both airway epithelial cell lines.

Next, in order to determine what factors were in complex with BRD8 to recruit it to chromatin we used HOMER to predict overrepresented transcription factor binding sites in the area under the ChIP-seq peaks. In both Calu-3 (Fig. 1A) and 16HBE14o- (Suppl. Fig. S-IIIA) cells, the most significant motifs were those for CCCTC-Binding Factor (CTCF) (Bell, West and Felsenfeld, 1999) and BORIS/CCCTC-Binding Factor Like (CTCFL)(Loukinov, Pugacheva, Vatolin et al., 2002). Also enriched at sites of BRD8 occupancy in both Calu-3 and 16HBE14o- cells were motifs for two steroid hormone receptors of potential relevance to BRD8 functions. The motif for Thyroid Hormone Receptor Beta (THRB) is substantially overrepresented (9.56% and 11.67% of targets compared to 3.52% of background) under BRD8 ChIP-seq peaks in Calu-3 and 16HBE14o- cells, respectively. Of note, the thyroid hormone receptor is a known BRD8 target (Monden et al., 1997). In both Calu-3 and 16HBE14o- cells the Estrogen Related Receptor Alpha (ERRA/ESRRA) motif is also enriched. ESRRA is most closely related to the estrogen receptor, and estrogen receptor alpha (ERA), is also a known BRD8 target (Monden et al., 1997,Gevry, Hardy, Jacques et al., 2009). Among other motifs that are over-represented under the BRD8 ChIP-seq peaks in both cell lines are binding sites for Zic family member 3 (*ZIC3*) (Ware, Peng, Zhu et al., 2004) and the BAF chromatin remodeling complex subunit BCL11A.

The contribution of BRD8 to the transcriptome of Calu-3 cells: identification of direct and indirect targets.

To detect genes that are directly or indirectly regulated by BRD8 in Calu-3 cells, RNA-seq was performed following siRNA-mediated depletion of BRD8. Three replicas of Calu-3 cells were transfected with BRD8 siRNA or non-targeting control (NC) siRNA. Efficacy of the siRNA-mediated reduction of BRD8 is shown by western blot in Fig. 2A. RNA-seq libraries were generated for each replicate and six libraries sequenced together on one lane of a HiSeq 4000, yielding ~ 4.5×10^7 reads per sample (Suppl. Table S-III). RNA-seq data were analyzed by DESeq2 to obtain estimates of the expression levels of transcripts. Of the six known BRD8 isoforms (Isoform-1, −2, −4 to −7)(Jiang et al., 2016), our RNA-seq analysis identified Isoform-1 and −4 (NM_006696 and NM_001164326) as the major isoforms in Calu-3 cells. Depletion of BRD8 in Calu-3 cells altered the expression of 3409 transcripts (Fig. 2B); 1800 were activated and 1609 were repressed by at least 1.3-fold (Suppl. Table S-IV, 1.5 fold change shown). Confirming our earlier data, *CFTR* expression

was significantly enhanced (>1.5 fold change) upon BRD8 depletion. We intersected the Entrez Gene ID for genes with Calu-3 BRD8 ChIP-seq peaks near the locus with the list of genes that were up- or down- regulated following siRNA-mediated BRD8-depletion in Calu-3 cells (Fig. 2B) and performed a gene ontology process enrichment analysis using DAVID (Huang da et al., 2009,Huang da et al., 2009). Among processes predicted from the up-regulated genes were response to wounding, response to organic substance, immune response, inflammatory response and defense response (Fig. 2C). Processes associated with down-regulated genes were related to the cell cycle and cell division (Fig. 2D). The full list of genes for the 10 most significant processes associated with up- or down-regulated genes are shown in Suppl. Tables S-V and S-VI, respectively. To further validate the RNA-seq data we measured the expression of 5 genes that were up-regulated upon BRD8 depletion and 5 that were down-regulated using RT-qPCR (Fig. 2E). Assays were performed on RNA extracted from independent samples of BRD8- or negative control- siRNA-treated Calu-3 cells. Among genes up-regulated upon BRD8 depletion that are involved in the immune response of the airway, C-X-C Motif Chemokine Ligand-6 (*CXCL6*, $P < 0.01$), defensin beta 1 (*DEFB1*, $P < 0.01$) and C-C Motif Chemokine Ligand-5 (*CCL5*, $P < 0.01$) were also significantly up-regulated in RT-qPCR assays (Fig. 2E). In contrast, the increase in C-X-C Motif Chemokine Ligand-17 (*CXCL17*) after BRD8-depletion did not reach significance, in part due to large inter-sample variation. Similarly, the C-C Motif Chemokine Ligand-2 (*CCL2*), which did not show altered abundance following BRD8-depletion in the RNA-seq data also showed no significant change by RT-qPCR analysis. Among genes down-regulated after BRD8-depletion, RT-qPCR assays confirmed a significant reduction in transcripts for Cell Division Cycle 25C (*CDC25C*, $P < 0.01$), Citron Rho-Interacting Serine/Threonine Kinase (*CIT*, $P < 0.001$), Centromere Protein F (*CENPF*, $P < 0.05$) and Cell Division Cycle Associated 2 (*CDCA2*, $P < 0.01$) (Fig. 2E). The decrease in expression of Abnormal Spindle Microtubule Assembly (*ASPM*) was not significant. We also confirmed the reduction in BRD8 expression ($P<0.0001$). These data suggest the RNA-seq data are robust and identify a role for BRD8 in regulating both the innate immune response and the cell cycle in airway epithelial cells. Further validation of these results in 16HBE14o- cells upon BRD8 depletion is shown in Figure S-V, where cell cycle genes are responsive to loss of BRD8. However, the observation that not all the immune response genes identified as BRD8 targets in Calu-3 cells are significantly altered in 16HBE14o- cells is likely due to their very low transcript abundance in this cell line.

Effect of siRNA-mediated BRD8-depletion on chemokine secretion and cell proliferation

Since immune-response genes were up-regulated following BRD8-depletion, we next measured the secretion of beta-defensin 1 (DEFB1), C-C motif chemokine 5 (CCL5) and C-X-C motif chemokine 2 (CXCL2) proteins from Calu-3 cells transfected with BRD8-siRNA or a non-targeting control sequence. BRD8-depleted Calu-3 cells secreted substantially more DEFB1 ($P < 0.001$), CCL5 ($P < 0.0001$) and CXCL2 ($P < 0.01$) protein into their growth media than control siRNA-transfected cells, as measured by ELISA (Fig. 3A). To determine whether the impact of BRD8 on these immune mediators was a direct effect, we examined the BRD8 ChIP-seq IDR data in Calu 3 cells. At the *DEFB1* locus multiple sites of BRD8 occupancy were evident, one at the promoter, one intronic, and both 5’ and 3’ (two) intergenic sites (all denoted by arrows, Fig. 3C), suggesting direct regulation of the gene.

Similarly, BRD8 occupancy was seen at the *CXCL2* promoter (Fig.3D) consistent with a direct regulatory mechanism.

Next, to determine whether siRNA-mediated depletion of BRD8 impaired the growth rate of Calu-3 cells, as might be predicted from the repression of cell cycle-related genes, we performed cell proliferation assays in a BioTek Lionheart FX automated microscope. Ten thousand Calu-3 cells were reverse-transfected with 5 pmol of negative control or BRD8 siRNAs and seeded into 96 well plates, in triplicate. Cells were fixed using methanol:acetic acid (3:1) every 24 hours post transfection to 120 hours and the cell number in each well was counted after DAPI staining. A reproducible inhibition of cell proliferation was evident by 72 after BRD8 depletion compared to non-targeting control, which is statistically significant at 96 and 120 hours (Fig. 3B), consistent with the gene expression data.

The BRD8 transcriptional network in airway epithelial cells

Our earlier work on the role of key transcription factors (TFs) in coordinating the function of the airway epithelium illustrates a complex network of interacting factors (Paranjapye et al., 2020,Fossum et al., 2014,Fossum et al., 2017). To determine how BRD8 integrates into this network, we first looked for TFs that might be its direct targets. To achieve this, the list of BRD8-regulated genes (DEGs upon BRD8-depletion) that have nearby BRD8 ChIP-seq peaks was intersected with ~ 1500 factors included in the Dharmacon siGENOME siRNA library for human TFs. Sixty five TFs (30 up-regulated and 35 down-regulated) with a greater than 1.5 fold change in expression after BRD8 depletion and nearby peaks of BRD8 occupancy were identified (Table I). Among up-regulated TFs is Forkhead box A1 (FOXA1), which we recently showed to have an important role in maintenance of airway epithelial barrier integrity (Paranjapye et al., 2020). As shown in Fig. 3E sites of BRD8 occupancy are seen upstream of the promoter for the FOXA1 gene, in the first intron, and also in the second exon. Several immune response-related TFs were also identified in the up-regulated gene list; NFKB inhibitor zeta (NFKBIZ) (Fig. 3F) (Totzke, Essmann, Pohlmann et al., 2006), Early growth response 2 (EGR2) (Singh, Miao, Symonds et al., 2017) CCAAT enhancer binding protein-alpha and -delta (CEBPA and CEBPD) (latter shown in Fig. 3G) (Balamurugan and Sterneck, 2013,Didon, Roos, Elmberger et al., 2010). Validation of the impact of BRD8-depletion on expression of these genes is shown in Supplementary Figure S-VI. In contrast, several genes encoding chromatin-remodeling factors were seen in the down-regulated upon BRD8-depletion list (Table 1). These include, SWI/SNF Related, Matrix Associated, Actin Dependent Regulator Of Chromatin, Subfamily A, Member 1(SMARCA1) and Helicase Like Transcription Factor (HLTF) which encode two members of the SWI/SNF family that regulate gene transcription by altering local chromatin structure. Also in this list are Remodeling and spacing factor 1 (RSF1), which encodes a nuclear protein component of the RSF chromatin-remodeling complex (Loyola, Huang, LeRoy et al., 2003). These data illustrate how the impact of BRD8 on the airway cell gene regulatory network may be amplified by modulating the expression level of other critical TFs.

Bifunctional Role of BRD8 as a Transcriptional activator or Repressor

Our initial interest in the function of BRD8 was as a repressor of the *CFTR* gene. However, the genome-wide data presented above documented similar numbers of genes that were

activated (1800) or repressed (1609) by at least 1.3-fold upon BRD8-depletion. To learn more about the regulatory mechanism whereby BRD8 impairs or enhances gene expression genome-wide, we intersected sites of BRD8 occupancy with the genomic location of repressive or active histone marks. ChIP-seq data generated using antibodies specific for repressive (H3K9me2, H3K27me3) or active histone marks (H3K27ac) were generated in Calu-3 cells. Figure 4 shows the intersection of sites of BRD8 occupancy with H3K9me2 (Fig. 4A), H3K27me3 (Fig.4B) and H3K27ac (Fig. 4C) using ChIPseeker (Yu et al., 2015). Though H3K9me2 and H3K27me3 were not substantially enriched at BRD8 sites, H3K27Ac was noticeably enhanced. Though we have not exhaustively examined other negative histone modifications in Calu-3 cells, these data suggest that the direct actions of BRD8, which coincide with sites of chromatin occupancy, are associated with activation of gene expression. The repressive activity of BRD8 observed on many loci may instead be an indirect effect coinciding with the activation of other repressive factors. This would appear to be the case for the repression of *CFTR*, as though BRD8 may be seen at the gene promoter in Calu-3 cell ChIP-seq data, this occupancy is inconstant.

Recruitment of CTCF at a subset of BRD8 binding sites.

In HOMER analysis of the BRD8 ChIP-seq data in Calu-3 cells (Fig 1A) and 16HBE14o- cells (Suppl. Fig S-III), the most over-represented motifs in both known and *de novo* predictions were CCCTC binding factor (CTCF) or BORIS/CTCFL. Since BRD8 is not predicted to bind directly to DNA, an association with CTCF/CTCFL could be an effective route to achieving chromatin proximity (Pena-Hernandez, Marques, Hilmi et al., 2015). To further explore the potential contribution of CTCF to the mechanism of action of BRD8, we performed ChIP-seq to map CTCF binding sites genome-wide in two biological replicates of Calu-3 cells. The efficacy of the ChIP-seq experiment is demonstrated by the HOMER analysis in Fig 1B, where more than 30% of target sequences contain a motif for CTCF or CTCFL. Next, peaks of occupancy from the BRD8 (9,768) and CTCF (16,412) ChIP-seq experiments in Calu-3 cells were intersected using ChIPseeker (Yu et al., 2015) and showed that ~70% of BRD8 sites overlapped a CTCF site (Fig. 1C), thus supporting the *in silico* predictions. Moreover, the genomic distribution of overlapping BRD8 and CTCF sites was similar to each factor independently (Fig. 1D-F). Inspection of the location of sites of BRD8 occupancy relative to the center of CTCF ChIP-seq peaks showed a strong correlation, though with an asymmetric curve leaning towards the 5’ side (Suppl. Fig. S-IV).

In order to reveal more details of the TFs that may be involved at coincident sites of BRD8 and CTCF occupancy a HOMER analysis was performed on this subset of BRD8 peaks (Suppl. Fig S-IIIB). As for the full set of BRD8 peaks in 16HBE14o- cells, THRB was among over-represented, known motifs in the coincident sites for BRD8 and CTCF occupancy in Calu-3 cells, as was ERRA, consistent with these hormone receptors being recruited to the regulatory complex.

Discussion

Mechanisms that regulate gene expression in the airway epithelium are central to how this tissue responds to the environment, both in normal and disease states. The role of

Bromodomain Containing 8 (BRD8) and its transcriptional network in the lung epithelium remains unexplored. Here, we reveal the BRD8 occupancy profile genome-wide in human lung epithelial cell lines and defined the contribution of BRD8 to their transcriptome. We show that BRD8 targets genes involved in the innate immune response. Consistent with this observation, siRNA-mediated depletion of BRD8 increased the secretion of antimicrobial peptide, Beta-defensin 1 and the chemotactic proteins; C-C Motif Chemokine 5 (CCL5) and C-X-C Motif Chemokine 2 (CXCL2) from Calu-3 cells. Inspection of over-represented motifs within BRD8 ChIP-seq peaks from two airway epithelial cell lines (Calu-3 and 16HBE14o-) consistently identified CCCTC-Binding Factor (CTCF) at the top of the list, and hence as a potential co-factor of BRD8. CTCF has a major role as an architectural protein involved in chromatin organization (Bonev and Cavalli, 2016,Ghirlando and Felsenfeld, 2016,Ong and Corces, 2014)}, though it may also modulate gene expression directly, by binding to transcription start sites (Nora, Goloborodko, Valton et al., 2017). To determine whether BRD8 and CTCF proteins co-localize genome-wide, we performed CTCF ChIP-seq in Calu-3 cells and intersected these data with our BRD8 occupancy profile. Around 40% of sites of CTCF occupancy overlapped a BRD8 binding site, suggesting a functionally significant coincidence between these elements. This hypothesis is supported by work that identified BRD8 as a CTCF interactor by mass spectrometry following CTCF immunoprecipitation in MDA-MB-435 breast cancer cells (Pena-Hernandez et al., 2015). CTCF also cooperates with another Bromodomain-containing protein, BRD2, in mouse T lymphocytes and erythroid cells (Hsu, Gilgenast, Bartman et al., 2017,Cheung, Zhang, Jaganathan et al., 2017). We compared the motifs over-represented within the BRD8 peaks that overlapped (BRD8-CTCF coincident) or did not overlap (BRD8-selective) a CTCF site. Of note, CTCF and BORIS/CTCFL remained the most significantly overrepresented motifs within both groups. Although BORIS/CTCFL can bind and compete with CTCF at a subset of sites (Pugacheva, Rivero-Hinojosa, Espinoza et al., 2015,Sleutels, Soochit, Bartkuhn et al., 2012) it is of very low abundance in both Calu-3 and 16HBE14o- cells, so CTCF is likely the main protein occupying these motifs in this cellular context. However, since ~30% of BRD8 sites did not overlap with peaks of CTCF binding in the Calu-3 ChIP-seq data, BRD8 probably also forms complexes with other factors that are recruited to chromatin.

Based upon known motif predictions (Suppl. Fig. S-IIIB), these factors likely include the hormone receptors, THRB and ERRA/ESRRA, which are both abundant transcripts in Calu-3 and 16HBE14o- cells and, based on biochemical protocols, were previously reported to interact with BRD8 (Monden et al., 1997,Gevry et al., 2009). Also of interest are motifs for different C2H2-type zinc finger protein family members including, Zic Family Member 3 (ZIC3), a known motif in BRD8-CTCF coincident sites (Suppl. Fig. S-IIIB) and ZIC1 and ZIC2 among *de novo* motifs in the BRD8-selective sites (Suppl. Fig. S-IIIC). Although ZIC1, −2 and −3 are important during development their role in the lung epithelium is unknown. ZIC1 and ZIC2 are robustly expressed in the two lung cell lines examined here, while ZIC3 is not.

Of relevance with respect to the dominant functions of BRD8 as an activating or repressive TF in airway epithelial cells, intersection of our ChIP-seq data for H3K27ac, H3K27me3 and H3K9me2 suggests that the strongest correlation of sites of BRD8 occupancy is with active chromatin (H3K27Ac).

BRD8 targets genes involved in the innate immune response

BRD8 directly repressed genes involved in the innate immune response. Of these, Beta-defensin 1 (DEFB1) encodes an antimicrobial protein found in the airway epithelium (Zhao, Wang and Lehrer, 1996) that participates in the resistance of the lung epithelium to microbial colonization (Laube, Yim, Ryan et al., 2006). Neutrophils are essential effector cells of the innate immune response and express chemokine receptor CXC chemokine receptor 2 (CXCR2) that binds chemokines including C-X-C Motif Chemokine Ligand-2 and −6 (CXCL2 and CXCL6) to facilitate neutrophil recruitment to the lung (Reutershan, Morris, Burcin et al., 2006,Nagarkar, Wang, Shim et al., 2009,Wareing, Shea, Inglis et al., 2007). The expression of both CXCL2 and CXCL6 was inhibited by BRD8 in Calu-3 cells. CXCL6 (also known as Granulocyte chemotactic protein 2 (GCP-2) can also bind to the CXC chemokine receptor 1 (CXCR1) on neutrophils {(Proost, Wuyts, Conings et al., 1993); (Wuyts, Van Osselaer, Haelens et al., 1997). BRD8 also repressed the expression of CCL5 (also known as RANTES), which attracts T lymphocytes, eosinophils and basophils expressing the C-C chemokine receptor type 5 (CCR5) receptor (Kameyoshi, Dorschner, Mallet et al., 1992,Schall, Bacon, Toy et al., 1990,Kuna, Reddigari, Schall et al., 1992,Mattoli, Ackerman, Vittori et al., 1995). Another chemokine inhibited by BRD8 was CXCL17, a potent chemoattractant for immature dendritic cells and blood monocytes to the lungs, which also exhibits strong antimicrobial activity (reviewed in (Choreno-Parra, Thirunavukkarasu, Zuniga et al., 2020)). The impact of BRD8 on the expression of innate immune response genes may also be amplified through its activation or repression of other transcription factors. Notably, we identified several genes encoding TFs that were direct targets of BRD8, including NFKB inhibitor zeta (*NFKBIZ*), Early growth response 2 (*EGR2*), CCAAT enhancer binding protein-alpha and -delta (*CEBPA* and *CEBPD*). NFKBIZ encodes a regulator of inflammatory genes activated through TLR/IL-1 receptor signaling and is known to regulate NF-kB transcription factor complexes (Totzke et al., 2006). EGR2 represses excessive immune activation in T lymphocytes (Singh et al., 2017). CEBPD encodes an important mediator of innate immunity (Balamurugan and Sterneck, 2013) and binds to DNA as a homodimer or as a heterodimer with the related protein, CEBPA. Lung-specific inactivation of CEBPA impairs mouse lung development and epithelial differentiation, with animals developing a severe pathological state similar to chronic obstructive pulmonary disease (Didon et al., 2010).

Role of BRD8 and the cell cycle

Consistent with the observation that depletion of BRD8 down-regulated cell cycle-related genes in the Calu-3 airway epithelial cell line, loss of BRD8 also impaired the growth rate of Calu-3 cells. Similarly, depletion of BRD8 by RNAi reduced the proliferation of other cell lines including colon (HCT-116 cells) (Lashgari et al., 2018,Yamaguchi, Sakai, Shimokawa et al., 2010,Yamada and Rao, 2009) and prostate (LnCAP cells) cancer cells (Jiang et al., 2016). In summary, our data show that BRD8 has both potent activating and repressive functions in coordinating a transcriptional network in airway epithelial cells. Most importantly, in terms of lung disease, BRD8 regulates both the innate immune response and cell proliferation in these cells. This is achieved by multiple mechanisms, some involving CTCF and others likely dependent upon the recruitment of other transcription factors and co-factors.

Supplementary Material

Refer to Web version on PubMed Central for supplementary material.

Acknowledgements

We thank Dr Pieter Faber and his staff at the University of Chicago Genomics Core for all deep sequencing). We also thank Dr. C.J. Ott for helpful discussion and Dr. J.L. Kerschner for generating reagents.

Funding

This work was supported by the National Institutes of Health [R01 HL094585; R01 HL117843;(AH); T32 GM008056 (AP)] and the Cystic Fibrosis Foundation [Harris 16G0, 15/17XX0 and 18P0]

References

[1]. Herriges M. and Morrisey EE, 2014. Lung development: orchestrating the generation and regeneration of a complex organ, Development. 141, 502–13. [PubMed: 24449833]

[2]. Paranjapye A, Mutolo MJ, Ebron JS, Leir SH and Harris A, 2020. The FOXA1 transcriptional network coordinates key functions of primary human airway epithelial cells, Am J Physiol Lung Cell Mol Physiol. 319, L126–L136. [PubMed: 32432922]

[3]. Fossum SL, Mutolo MJ, Yang R, Dang H, O'Neal WK, Knowles MR, Leir SH and Harris A, 2014. Ets homologous factor regulates pathways controlling response to injury in airway epithelial cells, Nucleic Acids Res. 42, 13588–98. [PubMed: 25414352]

[4]. Kerschner JL, Paranjapye A, Yin S, Skander DL, Bebek G, Leir SH and Harris A, 2020. A functional genomics approach to investigate the differentiation of iPSCs into lung epithelium at air-liquid interface, J Cell Mol Med.

[5]. Fossum SL, Mutolo MJ, Tugores A, Ghosh S, Randell SH, Jones LC, Leir SH and Harris A, 2017. Ets homologous factor (EHF) has critical roles in epithelial dysfunction in airway disease, J Biol Chem. 292, 10938–10949. [PubMed: 28461336]

[6]. Fujisawa T. and Filippakopoulos P, 2017. Functions of bromodomain-containing proteins and their roles in homeostasis and cancer, Nat Rev Mol Cell Biol. 18, 246–262. [PubMed: 28053347]

[7]. Perez-Salvia M. and Esteller M, 2017. Bromodomain inhibitors and cancer therapy: From structures to applications, Epigenetics. 12, 323–339. [PubMed: 27911230]

[8]. Monden T, Wondisford FE and Hollenberg AN, 1997. Isolation and characterization of a novel ligand-dependent thyroid hormone receptor-coactivating protein, J Biol Chem. 272, 29834–41. [PubMed: 9368056]

[9]. Mutolo MJ, Leir SH, Fossum SL, Browne JA and Harris A, 2018. A transcription factor network represses CFTR gene expression in airway epithelial cells, Biochem J. 475, 1323–1334. [PubMed: 29572268]

[10]. Nielsen MS, Petersen CM, Gliemann J. and Madsen P, 1996. Cloning and sequencing of a human cDNA encoding a putative transcription factor containing a bromodomain, Biochim Biophys Acta. 1306, 14–6. [PubMed: 8611617]

[11]. Hosoya T, Monden T, Fukabori Y, Hashimoto K, Satoh T, Kasai K, Yamada M. and Mori M, 2008. A novel splice variant of the nuclear coactivator p120 functions strongly for androgen receptor: characteristic expression in prostate disease, Endocr J. 55, 657–65. [PubMed: 18560202]

[12]. Jiang CY, Ruan Y, Wang XH, Zhao W, Jiang Q, Jing YF, Han BM, Xia SJ and Zhao FJ, 2016. MiR-185 attenuates androgen receptor function in prostate cancer indirectly by targeting bromodomain containing 8 isoform 2, an androgen receptor co-activator, Mol Cell Endocrinol. 427, 13–20. [PubMed: 26940039]

[13]. Monden T, Kishi M, Hosoya T, Satoh T, Wondisford FE, Hollenberg AN, Yamada M. and Mori M, 1999. p120 acts as a specific coactivator for 9-cis-retinoic acid receptor (RXR) on peroxisome proliferator-activated receptor-gamma/RXR heterodimers, Mol Endocrinol. 13, 1695–703. [PubMed: 10517671]

[14]. Couture JP, Nolet G, Beaulieu E, Blouin R. and Gevry N, 2012. The p400/Brd8 chromatin remodeling complex promotes adipogenesis by incorporating histone variant H2A.Z at PPARgamma target genes, Endocrinology. 153, 5796–808. [PubMed: 23064015]

[15]. Doyon Y, Selleck W, Lane WS, Tan S. and Cote J, 2004. Structural and functional conservation of the NuA4 histone acetyltransferase complex from yeast to humans, Mol Cell Biol. 24, 1884–96. [PubMed: 14966270]

[16]. Yu Z, Chen T, Mo H, Guo C. and Liu Q, 2020. BRD8, which is negatively regulated by miR-876–3p, promotes the proliferation and apoptosis resistance of hepatocellular carcinoma cells via KAT5, Arch Biochem Biophys. 693, 108550. [PubMed: 32860757]

[17]. Lashgari A, Fauteux M, Marechal A. and Gaudreau L, 2018. Cellular Depletion of BRD8 Causes p53-Dependent Apoptosis and Induces a DNA Damage Response in Non-Stressed Cells, Sci Rep. 8, 14089. [PubMed: 30237520]

[18]. Shen BQ, Finkbeiner WE, Wine JJ, Mrsny RJ and Widdicombe JH, 1994. Calu-3: a human airway epithelial cell line that shows cAMP-dependent Cl- secretion, Am J Physiol. 266(5 Pt 1). L493–501. [PubMed: 7515578]

[19]. Cozens AL, Yezzi MJ, Kunzelmann K, Ohrui T, Chin L, Eng K, Finkbeiner WE, Widdicombe JH and Gruenert DC, 1994. CFTR expression and chloride secretion in polarized immortal human bronchial epithelial cells, Am J Respir Cell Mol Biol. 10, 38–47. [PubMed: 7507342]

[20]. Leir SH and Harris A, 2011. MUC6 mucin expression inhibits tumor cell invasion, Exp Cell Res. 317, 2408–19. [PubMed: 21851820]

[21]. Dobin A, Davis CA, Schlesinger F, Drenkow J, Zaleski C, Jha S, Batut P, Chaisson M. and Gingeras TR, 2013. STAR: ultrafast universal RNA-seq aligner, Bioinformatics. 29, 15–21. [PubMed: 23104886]

[22]. Liao Y, Smyth GK and Shi W, 2014. featureCounts: an efficient general purpose program for assigning sequence reads to genomic features, Bioinformatics. 30, 923–30. [PubMed: 24227677]

[23]. Love MI, Huber W. and Anders S, 2014. Moderated estimation of fold change and dispersion for RNA-seq data with DESeq2, Genome Biol. 15, 550. [PubMed: 25516281]

[24]. Browne JA, Harris A. and Leir SH, 2014. An optimized protocol for isolating primary epithelial cell chromatin for ChIP, PLoS One. 9, e100099. [PubMed: 24971909]

[25]. Huang da W, Sherman BT and Lempicki RA, 2009. Bioinformatics enrichment tools: paths toward the comprehensive functional analysis of large gene lists, Nucleic Acids Res. 37, 1–13. [PubMed: 19033363]

[26]. Huang da W, Sherman BT and Lempicki RA, 2009. Systematic and integrative analysis of large gene lists using DAVID bioinformatics resources, Nat Protoc. 4, 44–57. [PubMed: 19131956]

[27]. Yu G, Wang LG and He QY, 2015. ChIPseeker: an R/Bioconductor package for ChIP peak annotation, comparison and visualization, Bioinformatics. 31, 2382–3. [PubMed: 25765347]

[28]. Bell AC, West AG and Felsenfeld G, 1999. The protein CTCF is required for the enhancer blocking activity of vertebrate insulators, Cell. 98, 387–96. [PubMed: 10458613]

[29]. Loukinov DI, Pugacheva E, Vatolin S, Pack SD, Moon H, Chernukhin I, Mannan P, Larsson E, Kanduri C, Vostrov AA, Cui H, Niemitz EL, Rasko JE, Docquier FM, Kistler M, Breen JJ, Zhuang Z, Quitschke WW, Renkawitz R, Klenova EM, Feinberg AP, Ohlsson R, Morse HC 3rd and Lobanenkov VV, 2002. BORIS, a novel male germ-line-specific protein associated with epigenetic reprogramming events, shares the same 11-zinc-finger domain with CTCF, the insulator protein involved in reading imprinting marks in the soma, Proc Natl Acad Sci U S A. 99, 6806–11. [PubMed: 12011441]

[30]. Gevry N, Hardy S, Jacques PE, Laflamme L, Svotelis A, Robert F. and Gaudreau L, 2009. Histone H2A.Z is essential for estrogen receptor signaling, Genes Dev. 23, 1522–33. [PubMed: 19515975]

[31]. Ware SM, Peng J, Zhu L, Fernbach S, Colicos S, Casey B, Towbin J. and Belmont JW, 2004. Identification and functional analysis of ZIC3 mutations in heterotaxy and related congenital heart defects, Am J Hum Genet. 74, 93–105. [PubMed: 14681828]

[32]. Totzke G, Essmann F, Pohlmann S, Lindenblatt C, Janicke RU and Schulze-Osthoff K, 2006. A novel member of the IkappaB family, human IkappaB-zeta, inhibits transactivation of p65 and its DNA binding, J Biol Chem. 281, 12645–54. [PubMed: 16513645]

[33]. Singh R, Miao T, Symonds ALJ, Omodho B, Li S. and Wang P, 2017. Egr2 and 3 Inhibit T-bet-Mediated IFN-gamma Production in T Cells, J Immunol. 198, 4394–4402. [PubMed: 28455436]

[34]. Balamurugan K. and Sterneck E, 2013. The many faces of C/EBPdelta and their relevance for inflammation and cancer, Int J Biol Sci. 9, 917–33. [PubMed: 24155666]

[35]. Didon L, Roos AB, Elmberger GP, Gonzalez FJ and Nord M, 2010. Lung-specific inactivation of CCAAT/enhancer binding protein alpha causes a pathological pattern characteristic of COPD, Eur Respir J. 35, 186–97. [PubMed: 19608583]

[36]. Loyola A, Huang JY, LeRoy G, Hu S, Wang YH, Donnelly RJ, Lane WS, Lee SC and Reinberg D, 2003. Functional analysis of the subunits of the chromatin assembly factor RSF, Mol Cell Biol. 23, 6759–68. [PubMed: 12972596]

[37]. Pena-Hernandez R, Marques M, Hilmi K, Zhao T, Saad A, Alaoui-Jamali MA, del Rincon SV, Ashworth T, Roy AL, Emerson BM and Witcher M, 2015. Genome-wide targeting of the epigenetic regulatory protein CTCF to gene promoters by the transcription factor TFII-I, Proc Natl Acad Sci U S A. 112, E677–86. [PubMed: 25646466]

[38]. Bonev B. and Cavalli G, 2016. Organization and function of the 3D genome, Nat Rev Genet. 17, 661–678. [PubMed: 27739532]

[39]. Ghirlando R. and Felsenfeld G, 2016. CTCF: making the right connections, Genes Dev. 30, 881–91. [PubMed: 27083996]

[40]. Ong CT and Corces VG, 2014. CTCF: an architectural protein bridging genome topology and function, Nat Rev Genet. 15, 234–46. [PubMed: 24614316]

[41]. Nora EP, Goloborodko A, Valton AL, Gibcus JH, Uebersohn A, Abdennur N, Dekker J, Mirny LA and Bruneau BG, 2017. Targeted Degradation of CTCF Decouples Local Insulation of Chromosome Domains from Genomic Compartmentalization, Cell. 169, 930–944 e22. [PubMed: 28525758]

[42]. Hsu SC, Gilgenast TG, Bartman CR, Edwards CR, Stonestrom AJ, Huang P, Emerson DJ, Evans P, Werner MT, Keller CA, Giardine B, Hardison RC, Raj A, Phillips-Cremins JE and Blobel GA, 2017. The BET Protein BRD2 Cooperates with CTCF to Enforce Transcriptional and Architectural Boundaries, Mol Cell. 66, 102–116 e7. [PubMed: 28388437]

[43]. Cheung KL, Zhang F, Jaganathan A, Sharma R, Zhang Q, Konuma T, Shen T, Lee JY, Ren C, Chen CH, Lu G, Olson MR, Zhang W, Kaplan MH, Littman DR, Walsh MJ, Xiong H, Zeng L. and Zhou MM, 2017. Distinct Roles of Brd2 and Brd4 in Potentiating the Transcriptional Program for Th17 Cell Differentiation, Mol Cell. 65, 1068–1080 e5. [PubMed: 28262505]

[44]. Pugacheva EM, Rivero-Hinojosa S, Espinoza CA, Mendez-Catala CF, Kang S, Suzuki T, Kosaka-Suzuki N, Robinson S, Nagarajan V, Ye Z, Boukaba A, Rasko JE, Strunnikov AV, Loukinov D, Ren B. and Lobanenkov VV, 2015. Comparative analyses of CTCF and BORIS occupancies uncover two distinct classes of CTCF binding genomic regions, Genome Biol. 16, 161. [PubMed: 26268681]

[45]. Sleutels F, Soochit W, Bartkuhn M, Heath H, Dienstbach S, Bergmaier P, Franke V, Rosa-Garrido M, van de Nobelen S, Caesar L, van der Reijden M, Bryne JC, van Ijcken W, Grootegoed JA, Delgado MD, Lenhard B, Renkawitz R, Grosveld F. and Galjart N, 2012. The male germ cell gene regulator CTCFL is functionally different from CTCF and binds CTCF-like consensus sites in a nucleosome composition-dependent manner, Epigenetics Chromatin. 5, 8. [PubMed: 22709888]

[46]. Zhao C, Wang I. and Lehrer RI, 1996. Widespread expression of beta-defensin hBD-1 in human secretory glands and epithelial cells, FEBS Letters. 396, 319–322. [PubMed: 8915011]

[47]. Laube DM, Yim S, Ryan LK, Kisich KO and Diamond G, 2006. Antimicrobial peptides in the airway, Curr Top Microbiol Immunol. 306, 153–82. [PubMed: 16909921]

[48]. Reutershan J, Morris MA, Burcin TL, Smith DF, Chang D, Saprito MS and Ley K, 2006. Critical role of endothelial CXCR2 in LPS-induced neutrophil migration into the lung, J Clin Invest. 116, 695–702. [PubMed: 16485040]

[49]. Nagarkar DR, Wang Q, Shim J, Zhao Y, Tsai WC, Lukacs NW, Sajjan U. and Hershenson MB, 2009. CXCR2 is required for neutrophilic airway inflammation and hyperresponsiveness in a mouse model of human rhinovirus infection, J Immunol. 183, 6698–707. [PubMed: 19864593]

[50]. Wareing MD, Shea AL, Inglis CA, Dias PB and Sarawar SR, 2007. CXCR2 is required for neutrophil recruitment to the lung during influenza virus infection, but is not essential for viral clearance, Viral Immunol. 20, 369–78. [PubMed: 17931107]

[51]. Proost P, Wuyts A, Conings R, Lenaerts JP, Billiau A, Opdenakker G. and Van Damme J, 1993. Human and bovine granulocyte chemotactic protein-2: complete amino acid sequence and functional characterization as chemokines, Biochemistry. 32, 10170–7. [PubMed: 8399143]

[52]. Wuyts A, Van Osselaer N, Haelens A, Samson I, Herdewijn P, Ben-Baruch A, Oppenheim JJ, Proost P. and Van Damme J, 1997. Characterization of synthetic human granulocyte chemotactic protein 2: usage of chemokine receptors CXCR1 and CXCR2 and in vivo inflammatory properties, Biochemistry. 36, 2716–23. [PubMed: 9054580]

[53]. Kameyoshi Y, Dorschner A, Mallet AI, Christophers E. and Schroder JM, 1992. Cytokine RANTES released by thrombin-stimulated platelets is a potent attractant for human eosinophils, J Exp Med. 176, 587–92. [PubMed: 1380064]

[54]. Schall TJ, Bacon K, Toy KJ and Goeddel DV, 1990. Selective attraction of monocytes and T lymphocytes of the memory phenotype by cytokine RANTES, Nature. 347, 669–71. [PubMed: 1699135]

[55]. Kuna P, Reddigari SR, Schall TJ, Rucinski D, Viksman MY and Kaplan AP, 1992. RANTES, a monocyte and T lymphocyte chemotactic cytokine releases histamine from human basophils, J Immunol. 149, 636–42. [PubMed: 1378073]

[56]. Mattoli S, Ackerman V, Vittori E. and Marini M, 1995. Mast cell chemotactic activity of RANTES, Biochem Biophys Res Commun. 209, 316–21. [PubMed: 7537040]

[57]. Choreno-Parra JA, Thirunavukkarasu S, Zuniga J. and Khader SA, 2020. The protective and pathogenic roles of CXCL17 in human health and disease: Potential in respiratory medicine, Cytokine Growth Factor Rev. 53, 53–62. [PubMed: 32345516]

[58]. Yamaguchi K, Sakai M, Shimokawa T, Yamada Y, Nakamura Y. and Furukawa Y, 2010. C20orf20 (MRG-binding protein) as a potential therapeutic target for colorectal cancer, Br J Cancer. 102, 325–31. [PubMed: 20051959]

[59]. Yamada HY and Rao CV, 2009. BRD8 is a potential chemosensitizing target for spindle poisons in colorectal cancer therapy, Int J Oncol. 35, 1101–9. [PubMed: 19787264]

Highlights

- Sites of Bromodomain Containing 8 (BRD8) occupancy genome-wide were mapped in human lung epithelial cell lines (Calu-3 and 16HBE14o-).
- CCCTC-Binding Factor (CTCF) and several hormone receptors were identified as predicted co-factors of BRD8.
- Following siRNA-mediated depletion of BRD8, differentially expressed genes with peaks of BRD8 occupancy nearby were subject to gene ontology process enrichment analysis.
- BRD8 targets are enriched for genes involved in the innate immune response and the cell cycle. Depletion of BRD8 increased the secretion of the antimicrobial peptide beta-defensin 1 and multiple chemokines, and decreased cell proliferation.

A Over-represented motifs under BRD8 ChIP-seq peaks in Calu-3 cells

Name	Known Motif	P-value	Rank	% of targets	% of background
CTCF		1e-5591	1	42.91 %	0.70 %
BORIS (CTCFL)		1e-4479	2	44.55 %	1.62 %
Bcl11a		1e-189	3	10.46 %	3.44 %
THRb		1e-144	4	9.56 %	3.52 %
NeuroD1		1e-129	5	10.69 %	4.48 %
Unknown element		1e-91	6	8.67 %	3.87 %
CTCF		1e-91	7	1.24 %	0.08 %
Zic3		1e-86	8	10.30 %	5.08 %
Tgif2		1e-82	9	20.58 %	13.17 %
Erra		1e-81	10	18.02 %	11.12 %

B Over-represented motifs under CTCF ChIP-seq peaks in Calu-3 cells

Name	Known Motif	P-value	Rank	% of targets	% of background
CTCF		1e-1843	1	29.95 %	0.48 %
BORIS (CTCFL)		1e-1572	2	34.70 %	1.39 %
THRB		1e-112	3	8.31 %	1.92 %
NeuroD1		1e-60	4	7.19 %	2.42 %
Unkown element		1e-56	5	6.70 %	2.25 %
ZBTB7		1e-54	6	18.03 %	10.12 %
CTCF		1e-51	7	0.87%	0.02 %

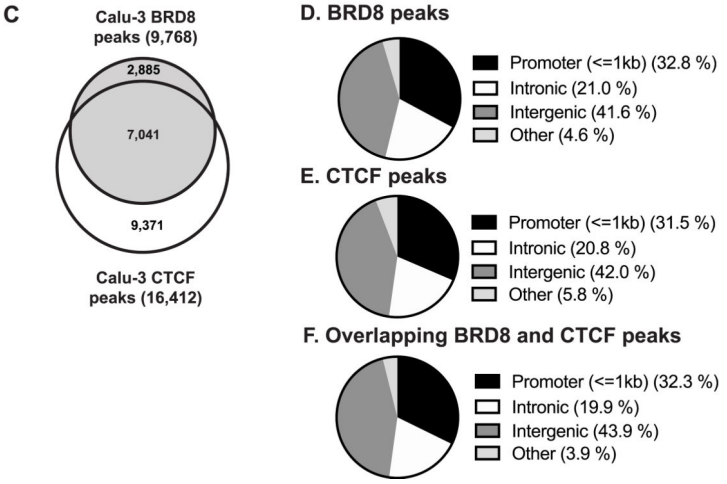

Figure 1. ChIP-seq identifies sites of BRD8 and CTCF occupancy genome-wide.

A, B, The top 7 enriched motifs under BRD8 (A) or CTCF (B) ChIP-seq peaks in Calu-3 cells. Motifs are ranked by their % incidence in target and background regions. C, Venn diagram showing the intersection of the BRD8- and CTCF- peaks in Calu-3 cells. D-F, Distribution of BRD8 peaks (D), CTCF peaks, (E) and overlapping BRD8 and CTCF peaks (F) in Calu-3 cells according to genomic features.

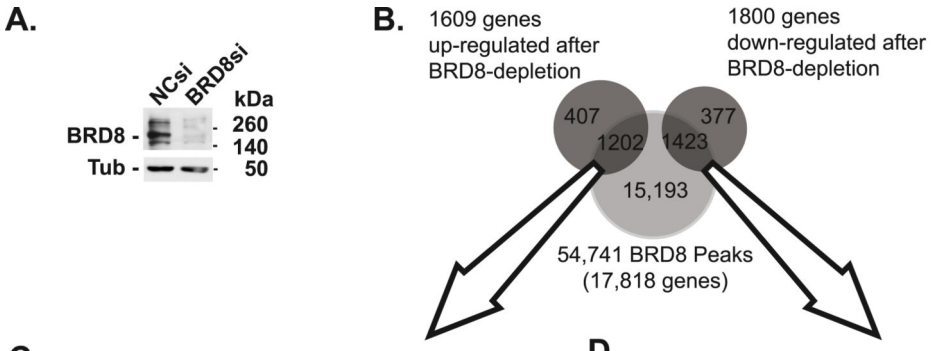

C.

Gene Ontology Term	Count	%	P value
Plasma membrane part	225	18	2E-09
Response to wounding	74	6	4E-09
Extracellular region	207	16	6E-09
Response to organic substance	89	7	4E-08
Extracellular region part	113	9	6E-08
Immune reponse	81	6	1E-06
Inflammatory response	46	4	4E-06
Extracellular space	81	6	5E-06
Defense response	71	6	1E-05
Enzyme inhibitor activity	39	3	2E-05
Plasma membrane	324	26	2E-05
Regulation of cell proliferation	84	7	3E-05
Negative regulation of cell proliferation	46	4	5E-05
Intrinsic to plasma membrane	122	10	6E-05
Response to cytokine stimulus	17	1	7E-05

D.

Gene Ontology Term	Count	%	P value
M Phase	88	8	7E-33
Cell cycle phase	99	9	1E-32
M Phase of mitotic cell cycle	72	7	2E-32
Cell cycle	140	13	3E-32
Nuclear division	71	6	5E-32
Mitosis	71	6	5E-32
Cell cycle process	116	11	9E-32
Mitotic cell cycle	92	8	1E-31
Organelle fission	71	6	8E-31
Cell division	79	7	2E-29
Chromosome	84	8	2E-21
Microtubule cytoskeleton	93	9	2E-21
Spindle	45	4	1E-20
Condensed chromosme	40	4	1E-18
Chromosome segregation	33	3	2E-18

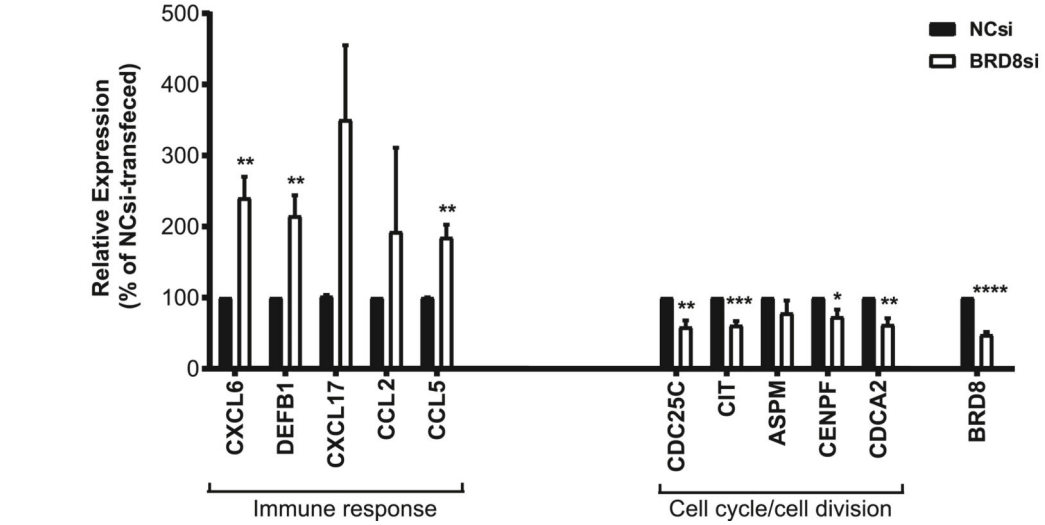

Fig. 2.

BRD8-depletion followed by RNA-sequencing reveals its role in regulating the transcriptome of Calu-3 cells. A, Efficacy of siRNA-mediated depletion of BRD8 in Calu-3 cells shown by western blot of cell lysates probed with an antibody specific for BRD8. B, Venn diagram showing the numbers of differentially expressed genes (after BRD8-depletion) with nearby BRD8 ChIP-seq peaks in Calu-3 cells. C, D, the top 15 statistically over-represented gene ontology processes of the genes with nearby BRD8 ChIP-seq peaks that were activated (C) or repressed (D) following BRD8-depletion in Calu-3 cells. (F) RT-

qPCR validation of differentially expressed genes in BRD8-siRNA-depleted and non-targeting (NC) siRNA-treated cells. Data are normalized to β−2 microglobulin (mean ± SD, n = 3) in comparison with NC siRNA (NC, black bars, BRD8 siRNA white bar). *P < 0.05, **P < 0.01 and ***P < 0.001 compared to NC siRNA-transfected cells.

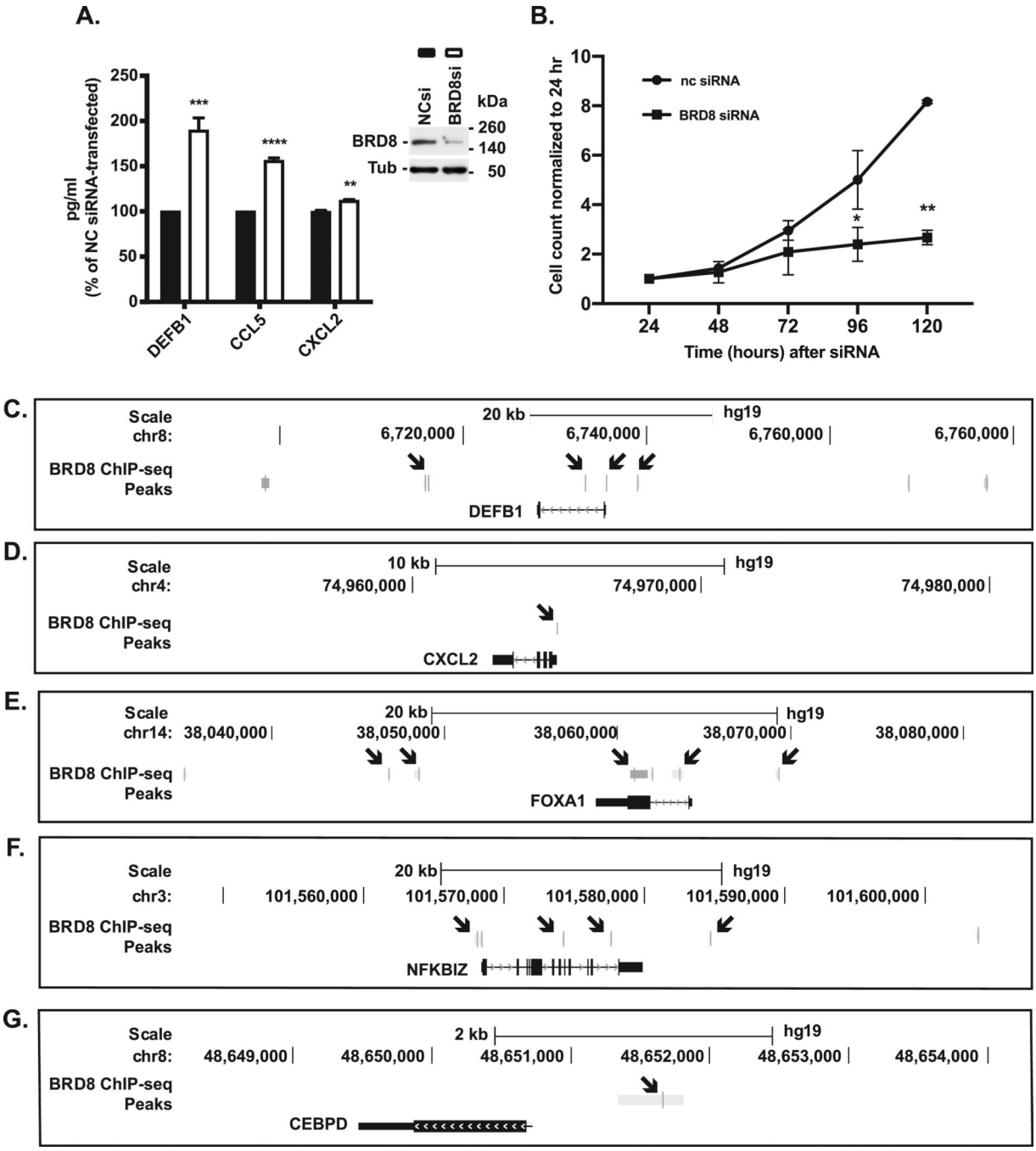

Figure 3. Effect of BRD8-depletion on airway epithelial function.

A, Secretion of beta-defensin 1 (DEFB1), C-C motif chemokine 5 (CCL5) and C-X-C motif chemokine 2 (CXCL2) into media conditioned by negative control (NC)- or BRD8-depleted Calu-3, quantified by colorimetric sandwich ELISA (n=3). **P < 0.01, ***P < 0.001 and ****P < 0.0001 compared to NC siRNA-transfected cells. B. Effect of BRD8-depletion on Calu-3 cell proliferation shown by using relative cell counts from 24 to 120 hr post transfection with Ambion siRNA (targeting BRD8 or a non-targeting control), (n=3). Error bars represent SEM. Statistics performed using an unpaired t-test (*P < 0.05, **P < 0.01). C-

G, Identification of sites of BRD8 occupancy at BRD8-regulated loci. Arrows denote the location of BRD8 ChIP-seq peaks in: (C) the *DEFB1* locus, (D) the *CXCL2* locus, (E) the *FOXA1* locus, (F) the *NFKBIZ* locus, (G) the *CEBPD* locus.

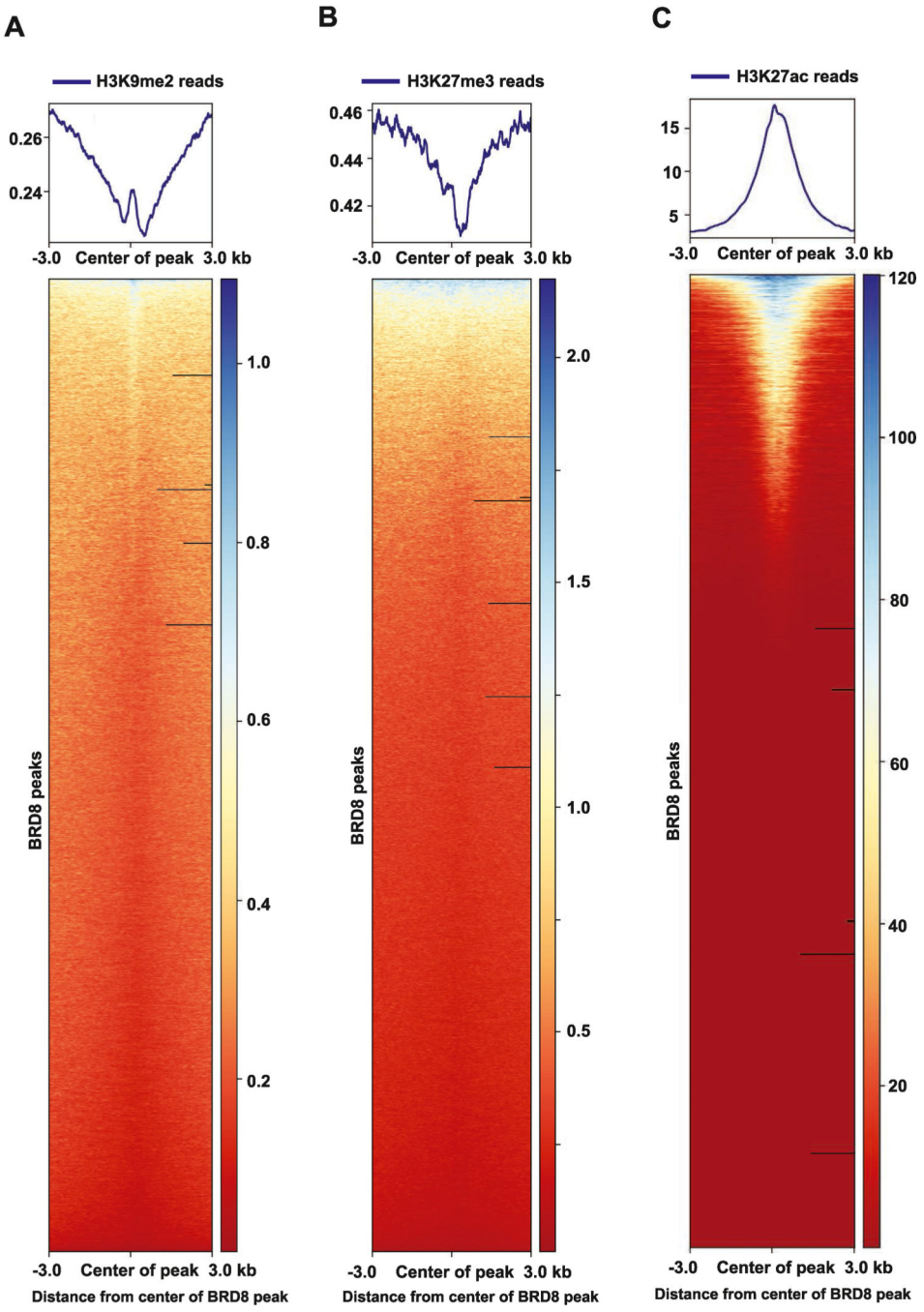

Figure 4. BRD8 occupancy coincides with active histone modification.

Intersection of BRD8 ChIP-seq peaks with ChIP-seq data for repressive (A, B) and active (C) histone marks. Heatmaps show the intersection of sites of BRD8 occupancy with (A) H3K9me2, (B) H3K27me3 and (C) H3K27ac using ChIPseeker with a window size of ± 3 kb from the center of the BRD8 peak.

Table 1.

Transcription Factor Genes that are up- (left side) or down- (right side) regulated following BRD8-depletion and have nearby BRD8 ChIP-seq binding sites

	Gene	base Mean	Actual Fold Change (Up)			Gene	base Mean	Actual Fold Change (Down)
1	CEBPA	27	4.3		1	RUNX3	147	4.1
2	NR1H4	471	3.5		2	BRD8	2050	2.5
3	KLF2	92	3.0		3	CBL	1420	2.0
4	POU2F3	174	3.0		4	FOXN3	266	1.9
5	EGR2	85	2.7		5	CAMK4	313	1.9
6	IRX3	21	2.6		6	IKZF3	285	1.8
7	RORC	272	2.5		7	ETS1	3857	1.8
8	MAF	28	2.4		8	ETV5	2311	1.7
9	EGR3	88	2.3		9	SHPRH	259	1.7
10	EGR1	2533	2.1		10	SCML1	618	1.7
11	IRX5	54	2.0		11	MED14	2544	1.7
12	FOS	938	1.9		12	SMARCA1	1410	1.7
13	CEBPD	652	1.9		13	PTTG1	2196	1.7
14	HES6	96	1.8		14	HMBOX1	260	1.6
15	SERTAD1	990	1.8		15	TRIP13	656	1.6
16	ANKRD1	237	1.8		16	HLTF	3899	1.6
17	NFE2	75	1.8		17	TFDP2	1234	1.6
18	FOXA3	1158	1.7		18	ANKRD26	545	1.6
19	MYB	133	1.7		19	FOSB	196	1.6
20	BCL3	615	1.6		20	TAF4B	345	1.5
21	FOXA1	757	1.6		21	RSF1	2045	1.5
22	BTG2	265	1.5		22	CLOCK	922	1.5
23	NOSTRIN	785	1.5		23	CIITA	147	1.5
24	TAX1BP3	195	1.5		24	HIVEP3	148	1.5
25	NFKBIZ	6424	1.5		25	ZNF496	382	1.5
26	MUC1	9793	1.5		26	ETV1	966	1.5
27	PAX8	864	1.5		27	HMGN5	792	1.5
28	ZFP36	1663	1.5		28	MYCN	228	1.5
29	MITF	1562	1.5		29	MEF2C	243	1.5
30	NMI	1403	1.5		30	PIR	318	1.5
					31	NR1D2	1678	1.5
					32	SHOX2	851	1.5
					33	HMGB2	2819	1.5
					34	SP4	1041	1.5
					35	RFX3	1006	1.5